LIGHT SCATTERING BY MARTIAN DUST ANALOGUES.

O. Muñoz, *Instituto de Astrofísica de Andalucía, CSIC, Granada, Spain. (olga@iaa.es)*, **J. Escobar-Cerezo, D. Guirado, F. Moreno,** *Instituto de Astrofísica de Andalucía, CSIC, Granada, Spain.*.

Introduction

Atmospheric dust plays a crucial role in the Martian radiative transfer budget. It is known that dust storms can modify temperature profile, dynamics, and chemical composition of the atmosphere. However, the quantification of the influence of dust particles on the atmosphere of Mars is far from trivial. Apart from its variable distribution in time and location, martian dust grains are irregular in shapes. This introduces a serious difficulty in the radiative transfer modelling. While the treatment of the scattering processes from spherical dust particles is straightforward using Lorenz-Mie theory, it becomes much more complicated, or even impossible, for realistic poly-dispersions of irregular dust particles.

In addition, in radiative transfer calculations, the vector nature of light is often replaced by its intensity or flux, i.e. polarization is ignored. We might note that under multiple scattering conditions (as is the case during large dust storms on Mars) even in the cases when only the radiance need to be computed, adopting a scalar representation of light induces significant, wavelength dependent, errors in the calculated planetary phase functions and geometric albedos ([Moreno (2002)], [Stam (2005)]). Thus, an appropriate representation of the scattering matrix of dust particles is mandatory under multiple scattering conditions. All in all, measurements of the full scattering matrices (including polarization) of realistic polydispersions of dust particles in the laboratory remain an extremely valuable tool.

In this work we present measurements of the full 4x4 scattering matrix as a function of the scattering angle of four Martian dust analog samples. The measurements has been performed at the IAA COsmic DUst LABoratory (CODULAB) ([Munoz et al. (2010)]), at three different wavelengths (488, 520, and 647 nm) covering the scattering angle range from 3 to 177 degrees.

Martian dust analogue samples

In our experiments four different analog samples have been analysed, namely, a palagonite (JSC Mars-1), montmorillonite, basalt, and calcite.

The palagonite sample is the < 1 mm size fraction of a palagonitic tephra (glassy volcanic ash altered at low temperatures) sample labelled as JSC Mars-1, where JSC stands for Johnson Space Center ([Allen (1998)]). Montmorillonite is the dominant clay mineral in bentonite, an altered volcanic ash. The montmorillonite sample used in this work is commercially available from WARD's Science, USA.

Apart from the palagonites and montmorillonite, we also present measurements for a basalt sample collected at Tenerife Island (Canary archipelago, Spain), which corresponds to the 1705 Arenas Negras volcanic eruption. The lava flow is defined as olivinic-pyroxenic basalt.

Although calcite is not a major component of the Martian surface, it is commonly considered to be particularly important for its link with climate evolution and water resources on Mars ([Booth (1978), Gooding (1978)]). The calcite sample studied in this work was obtained from limestone bulk material collected near Lecce, Italy ([Orofino (1998)]).

Shapes

At microscopic scales, a broad variety of shapes are present. In particular, the calcite and montmorillonite particles present rhomboidal- and flake-like structures with layered structures typical of sedimentary minerals. As an example in Figure 1, we present a Scanning Electronic Microscope image of the montmorillonite sample. For SEM images of the other analogues we refer to the Amsterdam-Granada Light Scattering Database (www.iaa.es/scattering) [Munoz et al. (2012)]. We might note that the SEM images are not necessarily representative of the size distribution of each sample. For that purpose we refer the reader to next subsection.

Size Distributions

The size distributions of the Martian analog samples are measured using a Mastersizer2000 particle sizer from Malvern Instruments. From the measured size distributions we calculate the values of the effective radii r_{eff} and effective variances v_{eff} as defined in [Hansen & Travis (1974)]. In Table 1 we present the calculated r_{eff} and v_{eff} for our samples. For a direct comparison with Martian dust we also include in Table 2 the values retrieved by [Tomasko (1999)]. As shown, our samples are characterised by a broad range of sizes, having, in many cases, r_{eff} and v_{eff} higher than those retrieved by [Tomasko (1999)] for Martian dust. However, it must be noted that the dust size distribution in the Martian atmosphere surely depends strongly on the weather conditions and altitude. In addition, our goal is to determine how the different physical parameters

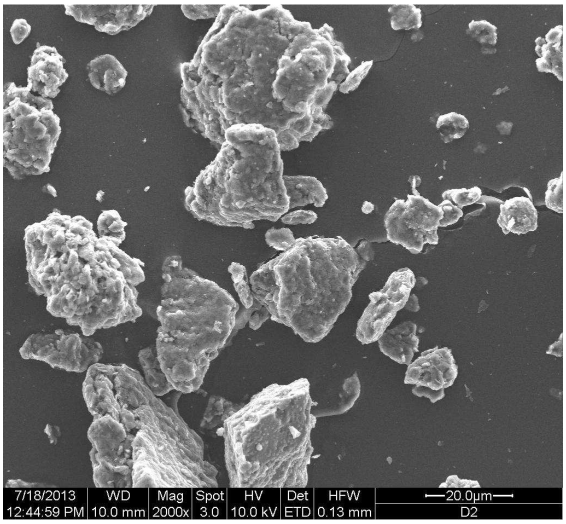

Figure 1: Scanning Electron Microscope images of montmorillonite. White bar denotes the scale of the image.

Table 1: Effective radii r_{eff} and effective variances v_{eff} of the Martian dust analog samples.

Sample	$r_{eff}[\mu m]$	v_{eff}
Basalt	2.9	15.1
	6.9	7.0
JSC0	17.2	2.4
	29.5	1.1
JSC200	15.5	2.8
	28.1	1.2
Calcite*	1.7	7.6
	3.3	4.9
Montmorillonite	1.8	1.6
	2.8	1.2
Martian dust [Tomasko (1999)]	1.6 ± 0.15	0.2-0.5 or more

of our Martian dust analogs might affect the measured scattering matrices.

Experimental Apparatus

The scattering matrices of our samples are measured at the IAA COsmic DUst LABoratory (CODULAB) located at the Instituto de Astrofísica de Andalucía, Granada, Spain. For a detailed description of the experimental apparatus, calibration process, and data acquisition we refer to [Munoz et al. (2010)]. Briefly, we use an Argon-Krypton laser as light source that can emits at three different wavelengths, 488, 520, and 647 nm. The laser beam passes through a polarizer and an electro-optic modulator. The modulated light is subsequently scattered by an ensemble of randomly oriented dust particles located in a jet stream produced by an aerosol generator. The scattered light passes through a quarter-wave plate and an analyzer (both optional) and is detected by a photomultiplier tube which moves along a ring. In this way a range of scattering angles from 3° to 177° is covered in the measurements. Another photomultiplier tube located at a fixed position is used to correct from fluctuations of the signal. We employ polarization modulation in combination with lock-in detection to obtain the entire four-by-four scattering matrix up to a constant. All matrix elements (except F_{11} itself) are normalized to F_{11}, that is, we consider F_{ij}/F_{11}, with i, j=1 to 4 with the exception of $i = j$ =1. The values of $F_{11}(\theta)$ are normalized so that they are equal to 1 at θ=30°. The function $F_{11}(\theta)$, normalized in this way, is called the phase function or scattering function in this work. The reliability of the apparatus has been tested by comparing measured scattering matrices of spherical water droplets at 488 nm, 520 nm and 647 nm with Lorenz-Mie computations ([Munoz et al. (2010)]). In addition, special tests have been performed to ensure that our experiment is performed under the single scattering regime ([Munoz et al. (2011)]). We also check that the measurements fulfil the Cloude coherency matrix test given in [Hovenier et al.(2004)] within the experimental errors at all measured scattering angles.

Comparison of the experimental data with derived phase functions in the Martian atmosphere.

In Fig. 2, we show the pseudo emission phase function retrieved from the Mars Colors Imager (MARCI band1) on board the Mars Reconnaissance Orbiter (MRO) observations [Wolff et al. (2009)]. The observations for Martian dust are presented together with Lorenz-Mie calculations for the same size distribution as retrieved by [Tomasko (1999)] (r_{eff}= 1.6 μm and v_{eff} equal to 0.2) and the refractive indices of the JSC sample (m=1.5+0.01i). Moreover, we show single Henyey-Greenstein phase functions for the asymmetry parameters retrieved for Martian dust at blue wavelengths g =0.65 ([OckertBell (1997)]), together with the experimental phase functions for basalt, and JSC0 samples at the corresponding wavelengths. To facilitate comparison with the laboratory measurements, in all cases the phase function is normalized to unity at 30 deg.

As shown in Fig. 2 none of the computed phase functions reproduce the observations for Mars. On the contrary, despite the differences in the size distributions of the Martian dust derived by Tomasko et al. (1999) and our Martian dust analogs, the agreement between observed and experimental phase functions for the Martian dust analogs is remarkable, especially in the case of the basalt sample. The main discrepancies are related to the forward diffraction peak that is highly dependent on the size of the particles.

Conclusions

In this work we present measurements of the full 4×4 scattering matrices as functions of the scattering angle of four Martian dust analogs: Basalt, JSC-1 Martian simulant, montmorillonite, and calcite. Tables of the measured scattering matrices will be available at the Amsterdam-Granada Light Scattering Database (www.iaa.es/scattering). Our measured phase functions have been compared with the retrieved phase functions for Martian dust from MARCI ([Wolff et al. (2010)]), and analytical Henyey-Greenstein phase functions. The measured phase functions at blue wavelengths of the Martian analogs closely mimic the phase functions retrieved using space-borne instrumentation ([Wolff et al. (2010)]). Further, the experimental data indicates that polarimetric color might be and indication of the composition of Martian dust. Therefore, spectro-polarimetric observations from Martian surface appear to be a powerful diagnostic tool to infer information on the physical properties of Martian dust.

References

[Allen (1998)] Allen, C. C., Morris, R. V., Jager, K. M., Golden, D. C., Lindstrom, D. J., Lindstrom, M. M. and Lockwood, J. P. 1998. Lunar and Plnaetary Science Conference, 29.

[Booth (1978)] Booth, M. C. and Kieffer, H. H. 1978. JGR, 83, 1809.

[Dabrowska et al (2015)] Dabrowska, D.D., Muñoz, O., Moreno, F., Ramos. J.L., Martinez-Frias, J., Wurm., G. 2015. Icarus, 250, 83.

[Gooding (1978)] Gooding, J. L. 1978. Icarus, 33, 483.

[Hansen & Travis (1974)] Hansen, J. E. and Travis, L. D. 1974. Space Sci. Rev. 16, 527. Gooding, J. L. 1978. Icarus, 33, 483.

[Hovenier et al.(2004)] Hovenier, J.W., van der Mee, C.V.M., and Domke, H. 2004, Transfer of polarized light in planetary atmospheres : Basic concepts and practical methods, (Kluwer/ Springer, Dordrecht)

[Moreno (2002)] Moreno, F. Muñoz, O., López-Moreno, J. J. Molina, A. and Ortiz, J. L.. 2002. Icarus, 156, 474.

[Munoz et al. (2010)] Muñoz, O. Moreno, F., Guirado, D., Ramos, J. L., López, A., Girela, F., Jerónimo, J. M., Costillo, L. P., and Bustamante, I. 2010. JQSRT, 111, 187-196.

[Munoz et al. (2011)] Muñoz, O. Moreno, F., Guirado, D., Ramos, J. L., Volten, H. and Hovenier, J.W. 2011. Icarus, 211, 894.

[Munoz et al. (2012)] Muñoz, O., Moreno, F., Guirado, D. and Dabrowska, D. D. 2012, JQSRT, 113, 565.

[OckertBell (1997)] Ockert-Bell, M. E., Bell, J. F., Pollack, J. B., McKay, C. P., and Forget, F. 1997. JGR, 102, 9039.

[Orofino (1998)] Orofino, V., Blanco, A., Fonti, S., Proce, R. and Rotundi, A. 1998. PSS, 46, 1659.

[Stam (2005)] Stam, D.M., Hovenier, J.W. 2005, A&A, 444, 275.

[Tomasko (1999)] Tomasko, M. G., Doose, L. R., Lemmon, M. Smith, P. H. and Wegryn, E. 1999. JGR, 104, 8987.

[Wolff et al. (2009)] Wolff, M. J., Smith, M. D., Clancy, R. T., Arvidson, R., Kahre, M., Seelos, F., Murchie, S., and Savijärvi, H. 2009. JGR, doi 10.1029/2009JE003350.

[Wolff et al. (2010)] Wolff, Clancy, R. T., Goguen, JD., malin, M., Cantor, B.A. 2010. Icarus, 208(1), 143.

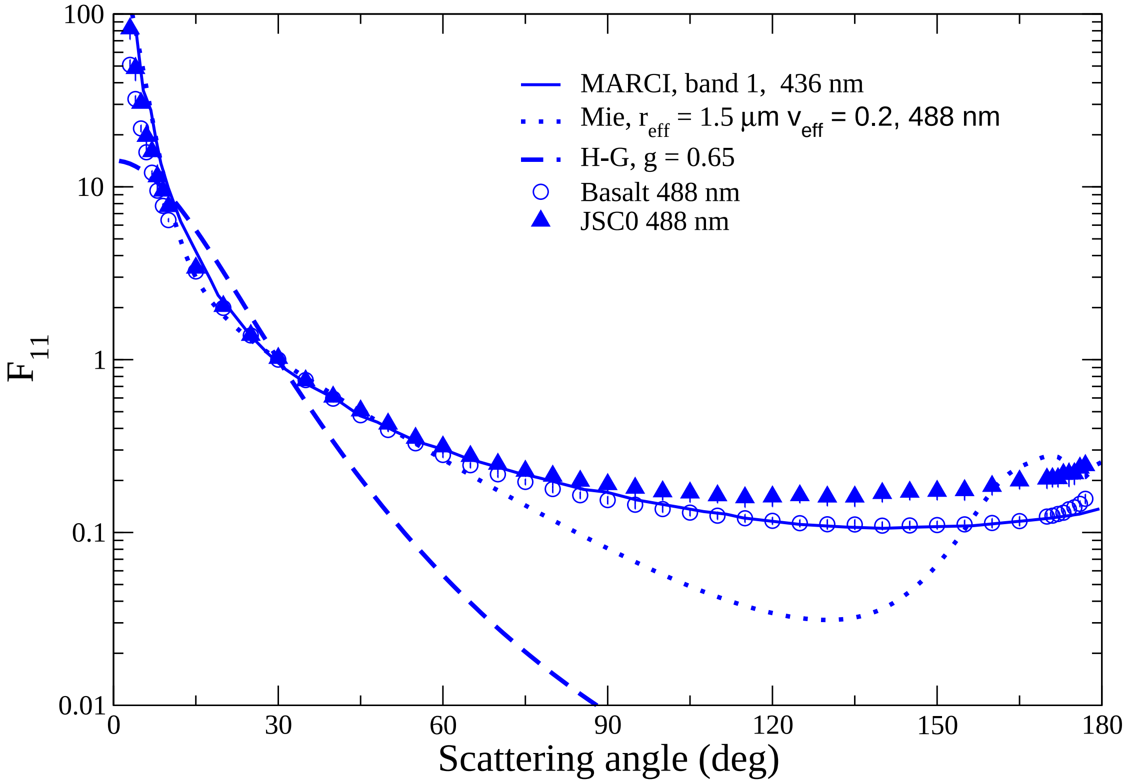

Figure 2: Pseudo Emission Phase Function constructed from MARCI band 1 (Wolff et al. 2010) at 436 nm (solid line) (top). We also present the analytical Henyey-Greenstein phase function for g= 0.65 (dashed line), and calculated phase functions for spheres (dotted line) together with our measurements for basalt, and JSC0 samples at 488 nm. After Dabrowska et al. 2015.